Supporting Information

Veelders et al. 10.1073/pnas.1013210108

Methods

Yeast Flocculation and Adhesive Growth Tests. Yeast strains used in this study are described in Table S1. Flocculation and adhesive growth test were measured in the nonflocculent and nonadhesive *flo11*Δ mutant yeast strain RH2662 (1) carrying appropriate *FLO5* and *FLO11* gene constructs on centromere-based plasmids (Table S1). Flocculation assays were performed according to reference (2–4). Agar and plastic adhesion tests were performed as previously described (5, 6). Standard yeast culture medium was prepared essentially as described (7).

Plasmid Construction. All plasmids used in this study are listed in Table S1. Crucial parts of all plasmids were verified by sequence analysis after construction. BHUM1323 was generated by PCR amplification of the whole *FLO5* gene from yeast chromosomal DNA (RH2754) using primers FLO5-5 and FLO5-6 and subsequent cloning of the resulting DNA fragment into the vector pCR-BLUNT II-TOPO (Invitrogen). BHUM1514 was obtained by amplification of a *FLO5* fragment encoding amino acids 23 to 271 using BHUM1323 as the template and the primer pair FLO5-AA23/FLO5-AA271, followed by cloning of the resulting fragment into the *Escherichia coli* expression vector pET-28a(+) (Merck) using restriction enzymes *Nde*I and *Xho*I. BHUM1301 carrying the *FLO11* promoter, the *FLO11* secretion signal sequence (amino acid 1 to 24) and the *FLO11* terminator was generated by whole vector PCR using plasmid pME2519 as a template and primers FLO11-1 and FLO11-4 followed by *Sac*I restriction digestion and ligation. BHUM1327 carrying a *FLO11* variant lacking the A domain (residues 25 to 213) was obtained by the same strategy using pME2519 as a template and the primer pair FLO11-5/FLO11-6. To construct BHUM1435 carrying *FLO5* (encoding residues 26 to 1075) fused to the *FLO11* signal sequence and driven by the *FLO11* promoter, an appropriate *FLO5* fragment was amplified by PCR from chromosomal DNA (RH2754) using primers FLO5-1 and FLO5-4 followed by insertion of the resulting *FLO5* fragment into the *Sac*I site of plasmid BHUM1301. BHUM1505 was generated by amplification of the *FLO5* ORF lacking the A domain (residues 272 to 1075) using the primer pair FLO5-2/FLO5-4 and chromosomal DNA of yeast strain RH2754 followed by insertion of the resulting fragment into the *Sac*I site of plasmid BHUM1301. Plasmid BHUM1437 carrying a *FLO5A-FLO11BC* fusion gene driven by the *FLO11* promoter was obtained by amplification of a *FLO5A* fragment (encoding residues 26 to 271) from chromosomal DNA (RH2754) using primers FLO5-1 and FLO5-3 and subsequent insertion of the resulting fragment into the *Sac*I site of plasmid BHUM1327. Plasmids BHUM1526, BHUM1528, BHUM1530, BHUM1532, BHUM1533, BHUM1535, BHUM1537, and BHUM1540, respectively, were obtained by PCR-based site-directed mutagenesis from plasmid BHUM1514 using the QuickChange Site-Directed Mutagenesis Kit (Stratagene) and appropriate *FLO5* primer pairs (Table S1) introducing the desired amino acid substitution(s). Using the same method, plasmids BHUM1567, BHUM1568, BHUM1570, BHUM1571, BHUM1573, and BHUM1581 were obtained by site-directed mutagenesis using the appropriate *FLO5* primer pair with the indicated amino acid substitution and BHUM1437 as the template. BHUM1583 and BHUM1585 were obtained by amplification of a mutated *FLO5A* fragment with primers FLO5-1 and FLO5-3 from BHUM1532 or BHUM1535, respectively, and subsequent insertion in the *Sac*I site of plasmid BHUM1327.

Polyclonal Anti-Flo5A Antibodies. Polyclonal rabbit anti-Flo5A antibodies were generated using $Flo5^{23-271}$ protein purified from *E. coli* (for production and purification see below) and a standard immunization procedure (Pineda-Antikörper-Service).

Immunofluorescence Microscopy. The presence of comparable amounts of Flo5A domain carrying proteins on cell surfaces was verified by immunofluorescence microscopy using specific polyclonal rabbit anti-Flo5A antibodies (Fig. 1*B* and Fig. S5*A*). Cultures of yeast strain RH2662 expressing the appropriate *FLO* gene constructs were grown in low fluorescence yeast medium (8) to an optical density of 1. Cells were harvested and washed twice in PBS/1% BSA prior to incubation for 1h at RT in PBS/1% BSA/1:10.000 rabbit anti-Flo5A antibodies. After three wash cycles in PBS/1% BSA, cells were incubated for 20 min at RT in PBS/1% BSA/1:20.000 secondary goat antirabbit DyLight™ 488 antibodies (Jackson ImmunoResearch Laboratories, Inc.), followed by three wash cycles with PBS/1% BSA. Fluorescent staining of cells was analyzed on a Zeiss Axiovert 200 M microscope using (*i*) differential interference microscopy (DIC) and (*ii*) fluorescence microscopy using a GFP filter set (AHF Analysentechnik AG). Cells were photographed with a Hamamatsu Orca ER digital camera and pictures were processed and analyzed using the Improvision Volocity software (Improvision). Fluorescence signals were integrated and quantified by the ImageJ software (9).

Synthesis of Oligomannosides. The mannopentaose *A*, and the mannotriose *B*, (Fig. S4) were synthesized as described (10, 11). Deprotection of the mannopentaose *A*, was carried out in aqueous methylamine. After removal of the volatiles the target compound Man5(D2-D3) was purified by gel filtration (1. Biogel P4, H_2O; 2. LH-20, MeOH). The trimannoside *B*, was deprotected using catalytic sodium methylate in absolute methanol. After neutralization with acetic acid, Man3(D1) mannotriose mimicking the D1-arm of the N-linked glycan, was purified by gel filtration (Biogel P4, H_2O). Both compounds were characterized by ESI-TOF-MS and 2-D NMR.

Recombinant Overproduction and Crystallization of Flo5A Domain. *E. coli* Origami2 (DE3) (Merck) carrying plasmid BHUM1514 were incubated in LB-medium with IPTG (40 μM f.c.) for 3 days at 12 °C. After lysis and clarification of the supernatant the protein was purified by Ni-NTA affinity chromatography (Qiagen) and subsequent size exclusion chromatography using Superdex 200 prep grade material (GE Healthcare) in AM-Buffer (20 mM Tris/HCl, pH 8.0, 200 mM NaCl).

Initial crystallization was performed using commercially available crystallization screens (Qiagen) with a Cartesian 4004 dispensing system (Genomic solutions) and yielded two different crystal forms. Crystals for structure determination were grown in 96-well crystallization plates (Innovadyne) using 300 nL of protein solution (25 mg/mL) and 300 nL of reservoir solution (100 mM Bis-tris propane, pH 7.5, 0.5 M NaCl, 20% PEG 4000) for crystal form I (space group: $P2_12_12_1$) and 300 nL of reservoir solution (100 mM ammonium citrate, pH 5.0, 15% PEG 3350) for crystal form II (space group: $P3_212$). Crystals of crystal form I were soaked in their mother liquor with 50 mM $GdAc_3$ added for SIRAS experiments. Substrate soakings were performed in the respective mother liquor with addition of 50 mM $CaCl_2$ and 50 mM of mannose, α-1,2- α-1,3-, α-1,6-mannobiose, the mannotriose Man3(D1) or the mannopentaoses

Man5(D2-D3) and Man5(core). Also, carbohydrate soakings were carried out at a concentration of 20% mannose or 40% glucose, where the carbohydrates served both as substrate and as cryoprotectant. Otherwise, crystals were frozen in liquid nitrogen in their mother liquor with an addition of 15% glycerol.

Datasets for structure solution were recorded on a mar345 area detector system (Marresearch) using a FR591 rotating anode (Bruker/Nonius) as X-ray source. Using the anomalous signal of the incorporated gadolinium initial SIRAS-phasing by SHELX-CDE (12) succeeded. Crystal form II was solved by molecular replacement with the previously obtained Flo5A model. Further datasets of native and substrate soaked crystals were recorded at beamlines ID14-2, ID14-4 and ID29 of ESRF, Grenoble. Data processing was carried out using XDS and the CCP4 package (13, 14), final refinement was performed via REFMAC5 (15) and Coot (16).

The secondary structure of the Flo5A domain was assigned by STRIDE (17) giving rise to 19 β-strands organized either in the large PA14-like β-sandwich or the therein inserted Flo5 subdomain (see Fig. S2*A*, residues 35–37, 39–45, 69–76, 82–83, 86–89, 92–95, 101–103, 105–107, 111–113, 136–144, 150–156, 162–167, 190–192, 205–210, 216–224, 229–231, 233–236, 242–244, 251–254). Figures were generated using the program PYMOL 1.0 (18). Electrostatic surface potentials of the Flo5A domain were calculated by APBS (19) using an ionic strength of 0.1 M and mapped onto the molecular surface generated by PYMOL using a probe radius of 1.4 Å.

Fluorescence Titration of Flo5A Domain. Fluorescence spectroscopy was performed with Flo5A in phosphate buffer (0.1 M, pH 5). 500 μL of protein solution (250 μg/mL Flo5A, 10 mM $CaCl_2$) were titrated with substrate solution [250 μg/mL Flo5A, 10 mM $CaCl_2$ and 125 mM mannose, 20 mM α-1,2-mannobiose, 20 mM Man3(D1) or 20 mM Man5(D2-D3), respectively]. The intrinsic fluorescence of tryptophane was excited at a wavelength of 295 nm, the fluorescence maxima were observed at 342–345 nm and the fluorescence quench was recorded. The measurements were repeated multiple times, the values averaged and fitted with Prism5 (GraphPad).

1. Braus GH, Grundmann O, Brückner S, Mösch HU (2003) Amino acid starvation and Gcn4p regulate adhesive growth and *FLO11* gene expression in *Saccharomyces cerevisiae*. *Mol Biol Cell* 14:4272–4284.
2. Bester MC, Pretorius IS, Bauer FF (2006) The regulation of *Saccharomyces cerevisiae FLO* gene expression and Ca^{2+}-dependent flocculation by Flo8p and Mss11p. *Curr Genet* 49:375–383.
3. Miki BLA, Poon NH, James AP, Seligy VL (1982) Possible mechanism for flocculation interactions governed by gene *FLO1* in *Saccharomyces cerevisiae*. *J Bacteriol* 150:878–889.
4. Miki BLA, Poon NH, Seligy VL (1982) Repression and induction of flocculation interactions in *Saccharomyces cerevisiae*. *J Bacteriol* 150:890–899.
5. Roberts RL & Fink GR (1994) Elements of a single MAP kinase cascade in *Saccharomyces cerevisiae* mediate two developmental programs in the same cell type: Mating and invasive growth. *Genes Dev* 8:2974–2985.
6. Reynolds TB, Fink GR (2001) Bakers' yeast, a model for fungal biofilm formation. *Science* 291:878–881.
7. Guthrie C, Fink GR, eds (1991) *Guide to Yeast Genetics and Molecular Biology* (Academic Press, San Diego), Vol 194.
8. Sheff MA, Thorn KS (2004) Optimized cassettes for fluorescent protein tagging in *Saccharomyces cerevisiae*. *Yeast* 21:661–670.
9. Abramoff MD, Magelhaes PJ, Ram SJ (2004) Image processing with ImageJ. *Biophot Int* 11:36–42.
10. Schratt X, Unverzagt C (2005) Synthesis of an N-glycan decasaccharide of the hybrid type. *Tetrahedron Lett* 46:691–694.
11. Varon D, Lioy E, Patarroyo ME, Schratt X, Unverzagt C (2002) Synthesis of mannosyl and oligomannosyl threonine building blocks found on the mycobacterium tuberculosis 45 kDa MPT 32 glycoprotein. *Aust J Chem* 55:161–165.
12. Sheldrick GM (2008) A short history of SHELX. *Acta Crystallogr A* 64:112–122.
13. Kabsch W (2010) XDS. *Acta Crystallogr D* 66:125–132.
14. CCP4 (1994) The CCP4 suite: Programs for protein crystallography. *Acta Crystallogr D* 50:760–763.
15. Murshudov GN, Vagin AA, Dodson EJ (1997) Refinement of macromolecular structures by the maximum-likelihood method. *Acta Crystallogr D* 53:240–255.
16. Emsley P, Cowtan K (2004) COOT: Model-building tools for molecular graphics. *Acta Crystallogr D* 60:2126–2132.
17. Heinig M, Frishman D (2004) STRIDE: A web server for secondary structure assignment from known atomic coordinates of proteins. *Nucleic Acids Res* 32:W500–W502.
18. DeLano WL (2002) The PyMOL molecular graphics system. (DeLano Scientific LLC, http://www.pymol.org, San Carlos, CA).
19. Baker NA, Sept D, Joseph S, Holst MJ, McCammon JA (2001) Electrostatics of nanosystems: Application to microtubules and the ribosome. *Proc Natl Acad Sci USA* 98:10037–10041.

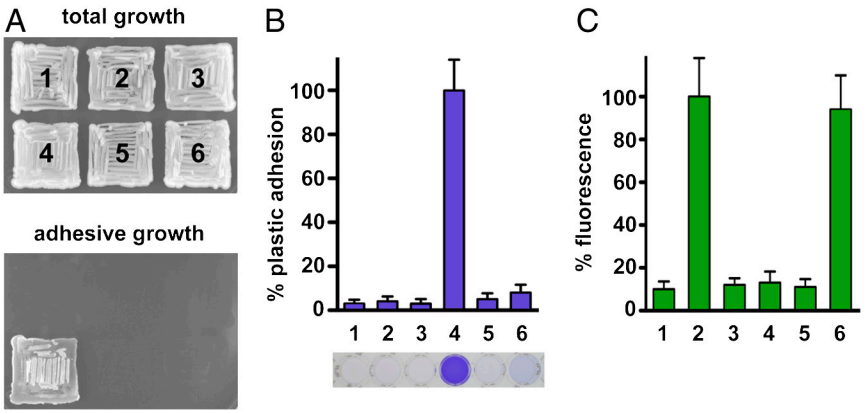

Fig. S1. Cell-surface adhesion mediated by different *FLO5* and *FLO11* constructs (numbering refers to Fig. 1*A*) expressed in the nonflocculating and nonadhesive Σ1278b *flo11*Δ mutant strain RH2662. (*A*) Agar-adhesion was determined after growth on solid medium. Agar plates were photographed before (total growth) and after (adhesive growth) removal of nonadhesive cells by a wash assay. (*B*) Adhesion to polystyrene plastics was measured and quantified as previously described (6). (*C*) Quantification of cell-surface exposed Flo5A domain using immunofluorescence microscopy and anti-Flo5A polyclonal antibody was performed on cultures used in *B* and on cultures used in Fig. 1 *B* and *C* in the main text.

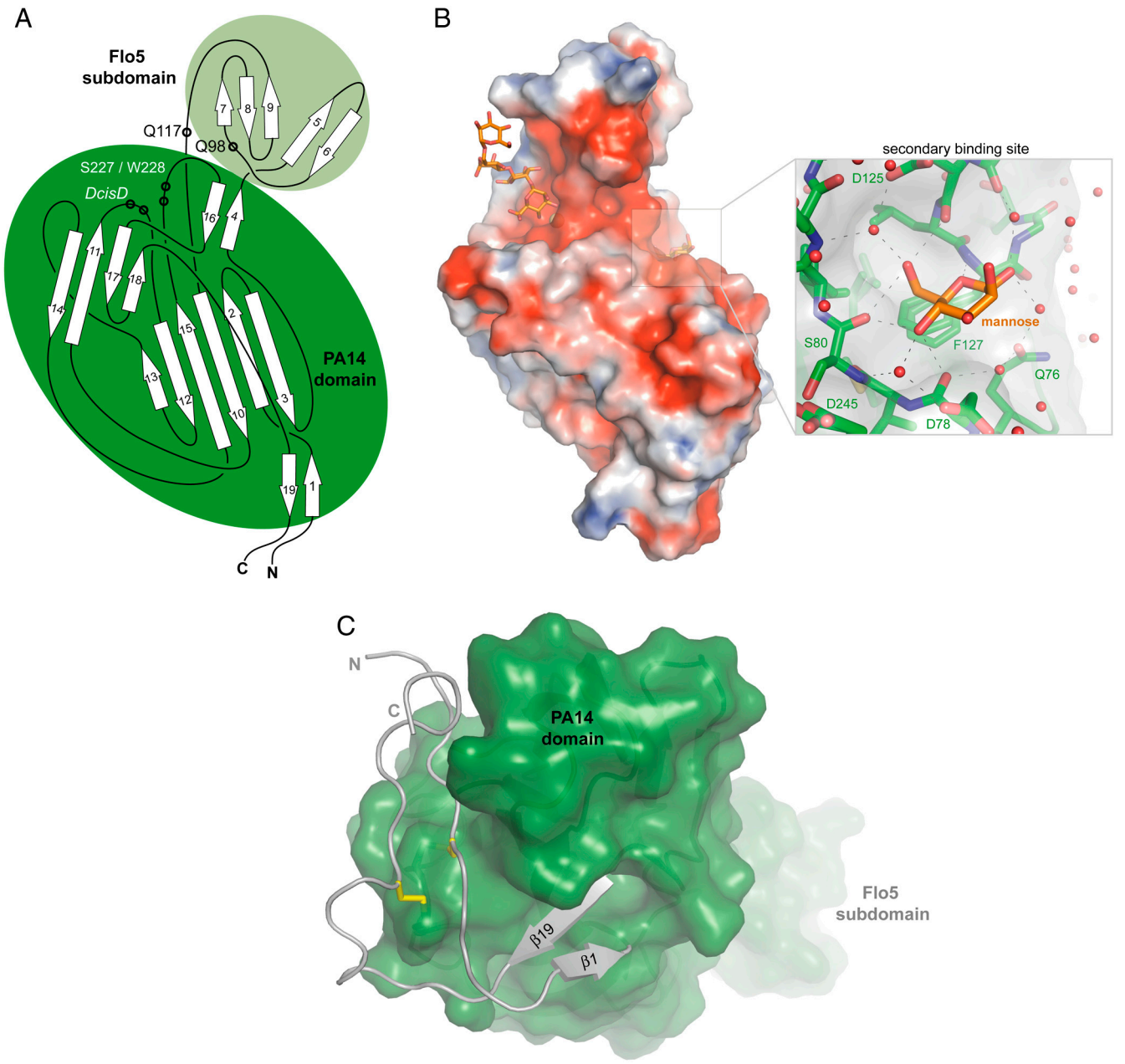

Fig. S2. Structural characteristics of the Flo5A domain. (*A*) Protein topology diagram showing the PA14-like domain (green) and the five-stranded Flo5 subdomain (light green). (*B*) Surface charge distribution (red: −5 kT/*e*; blue: +5 kT/*e*) as calculated by APBS and location of the primary and secondary carbohydrate-binding sites occupied by either the Man5(D2-D3) mimic or mannose (orange). The inlay shows a detailed view of the secondary sugar-binding site occupied by mannose. In this site, the binding of glucose has been observed as well, when crystals were soaked in 2 M glucose as cryoprotectant. (*C*) L-shaped region formed by the N and C termini of Flo5A (gray). The disulfide bridges linking the termini to the β12–β13 loop of the PA14-like core domain are highlighted in yellow.

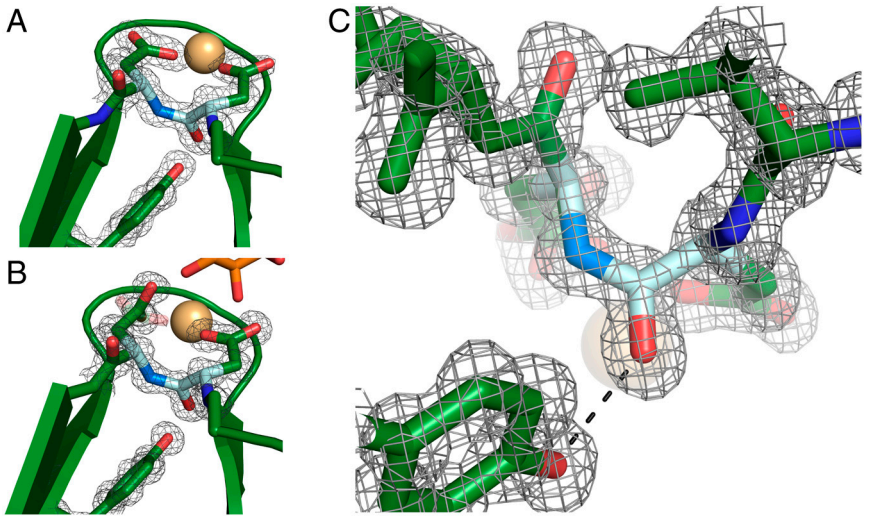

Fig. S3. Structural features of the *DcisD* motif. (*A*) The *DcisD* motif without bound carbohydrates in the presence of calcium (golden). The aspartates are horizontally aligned. The distance between the liganded OD1 atoms of the two aspartates is 2.3 Å. (*B*) *DcisD* motif with bound mannose. D161 is flipped by approximately 70°. The residual occupancy of the unflipped aspartate carboxylate is about 10% (semitransparent sticks). The distance between D160 and D161 in its horizontal state is here about 2.0 Å. (*C*) The *cis*-peptide bond ($\omega = 13.4°$) is highlighted and forms a hydrogen bond to Y222 (dashed line, 2.7 Å). The shown SIGMAA-weighted $2F_{obs}$-F_{calc} electron density maps are contoured at 1.5 σ (absolute level: 0.66 $e^-/Å^3$ in *A* and 0.67 $e^-/Å^3$ in *B* and *C*, respectively).

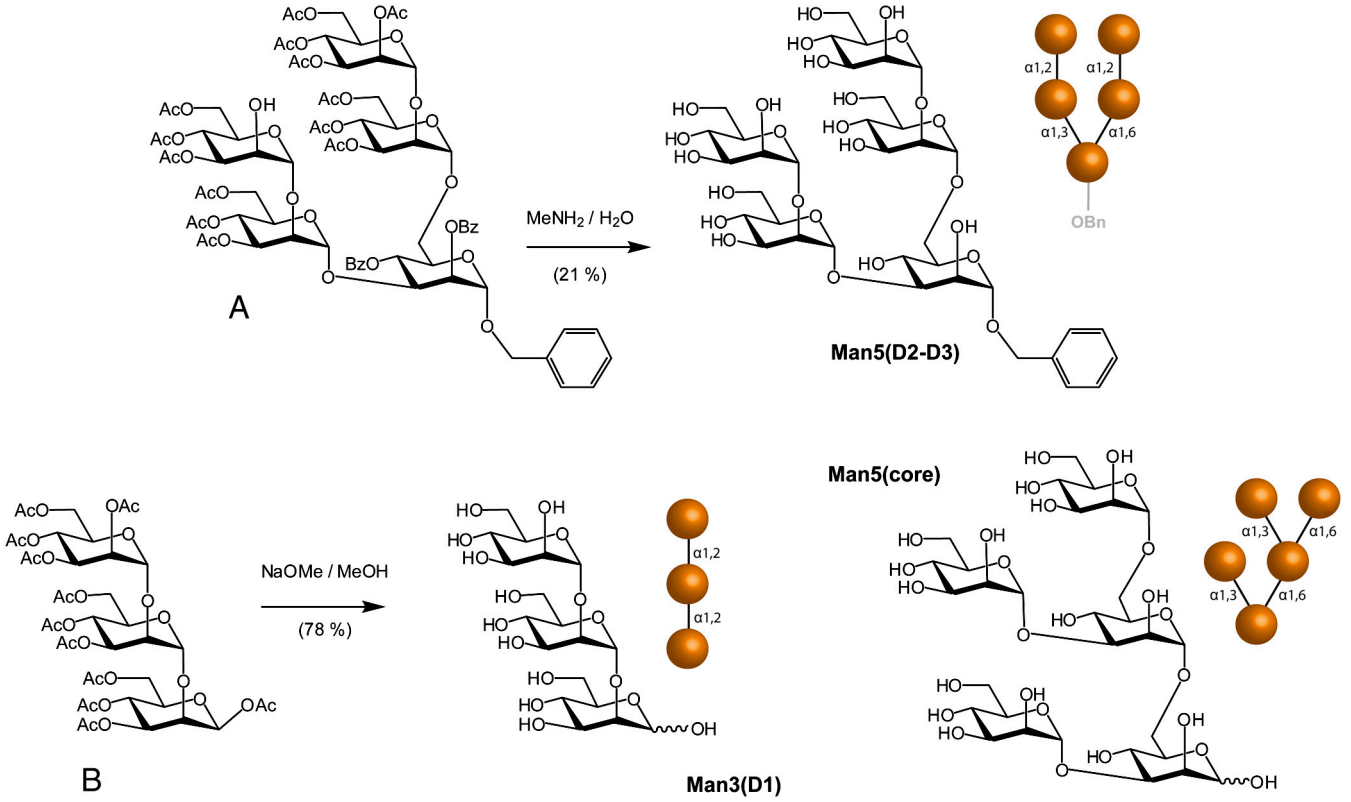

Fig. S4. Synthesis and chemical formulas of high-mannose oligosaccharides. Only the final deprotection steps for the synthesis of Man5(D2-D3) and the D1-arm mimic Man3(D1) using the precursors *A* and *B* are shown. For comparison the nonbinding mannopentaose mimicking the core of the N-linked glycan, Man5(core), is shown on the right.

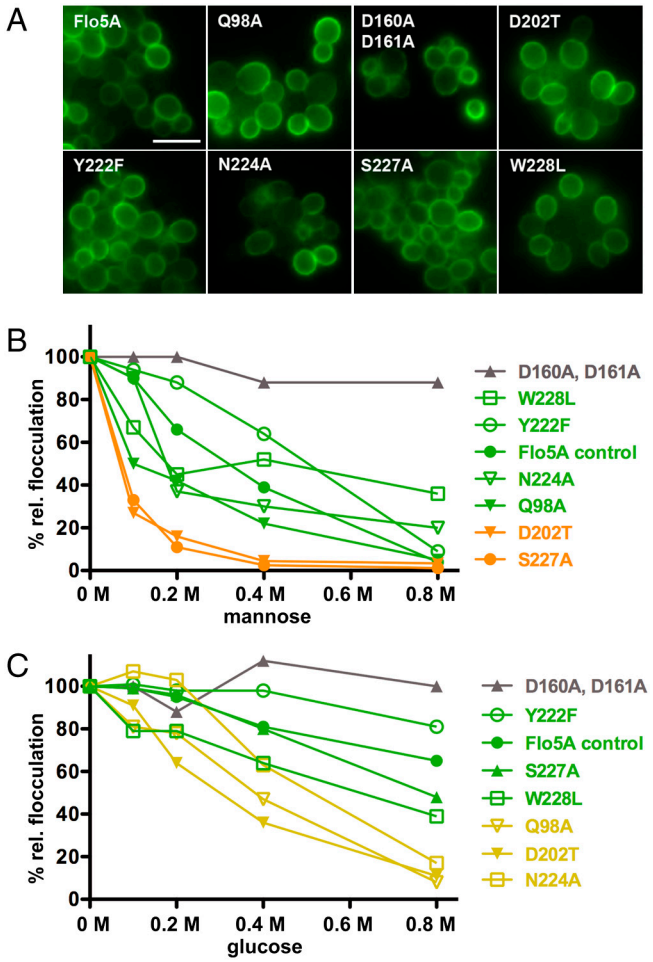

Fig. S5. Expression and functionality of different Flo5A variants. (*A*) The presence of different Flo5A variants on the yeast cell surface was shown by immunofluorescence microscopy using specific anti-Flo5A antibodies. The bar indicates 10 μm. Relative sensitivity of different Flo5A variants against increasing concentrations of mannose (*B*), and glucose (*C*), was determined by in vivo flocculation assays with yeast strains expressing the indicated *FLO5A* domain. Green curves represent wild-type-like behavior, orange and yellow curves represent mutants with increased sensitivity to mannose or glucose, respectively. The D160A, D161A mutant (gray) showed no flocculation.

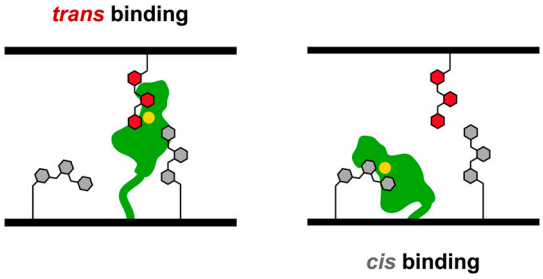

Fig. S6. Model for *trans* and *cis* ligand-binding by FloA domains. The primary ligand-binding site of FloA (green) can interact with terminal α-1,2-mannobiose residues present either in *trans* (red) or in *cis* (gray) depending on Ca^{2+} (yellow). The secondary ligand-binding site of FloA might stabilize *trans*-interactions of the domain by binding to mannose residues present in *cis*.

Table S1. Strains and DNA primers used in this study

Yeast strains

Strain	Genotype	Source
RH2662	*MAT***a** *flo11*Δ::*kanR ura3-52lala*	(1)
RH2754	*MAT***a** *ura3-52 leu2*::*hisG his3*::*hisG trp1*::*hisG*	(17)

Plasmids

Plasmid	Genotype	Source
BHUM1301	P_{FLO11}-*FLO*11$^{1-24}$-T_{FLO11} in YCplac33	This work
BHUM1323	P_{FLO5}-*FLO*5-T_{FLO5} in pCR-BLUNT II-TOPO	This work
BHUM1327	P_{FLO11}-*FLO*11$^{1-25}$-*FLO*11$^{214-1360}$-T_{FLO11} in YCplac33	This work
BHUM1435	P_{FLO11}-*FLO*11$^{1-24}$-*FLO*5$^{26-1075}$-T_{FLO11} in YCplac33	This work
BHUM1437	P_{FLO11}-*FLO*11$^{1-25}$-*FLO*5$^{26-271}$-*FLO*11$^{214-1360}$-T_{FLO11} in YCplac33	This work
BHUM1505	P_{FLO11}-*FLO*11$^{1-24}$-*FLO*5$^{272-1075}$-T_{FLO11} in YCplac33	This work
BHUM1514	*FLO*5$^{23-271}$ in pET-28a(+)	This work
BHUM1526	*FLO*5$^{23-271,D202T}$ in pET-28a(+)	This work
BHUM1528	*FLO*5$^{23-271,Y222F}$ in pET-28a(+)	This work
BHUM1530	*FLO*5$^{23-271,N224A}$ in pET-28a(+)	This work
BHUM1532	*FLO*5$^{23-271,Q98A}$ in pET-28a(+)	This work
BHUM1533	*FLO*5$^{23-271,D160A,D161A}$ in pET-28a(+)	This work
BHUM1535	*FLO*5$^{23-271,K194A}$ in pET-28a(+)	This work
BHUM1537	*FLO*5$^{23-271,W228L}$ in pET-28a(+)	This work
BHUM1540	*FLO*5$^{23-271,S227A}$ in pET-28a(+)	This work
BHUM1567	P_{FLO11}-*FLO*11$^{1-25}$-*FLO*5$^{26-271,D160A,D161A}$-*FLO*11$^{214-1360}$-T_{FLO11} in YCplac33	This work
BHUM1568	P_{FLO11}-*FLO*11$^{1-25}$-*FLO*5$^{26-271,D202T}$-*FLO*11$^{214-1360}$-T_{FLO11} in YCplac33	This work
BHUM1570	P_{FLO11}-*FLO*11$^{1-25}$-*FLO*5$^{26-271,Y222F}$-*FLO*11$^{214-1360}$-T_{FLO11} in YCplac33	This work
BHUM1571	P_{FLO11}-*FLO*11$^{1-25}$-*FLO*5$^{26-271,S227A}$-*FLO*11$^{214-1360}$-T_{FLO11} in YCplac33	This work
BHUM1573	P_{FLO11}-*FLO*11$^{1-25}$-*FLO*5$^{26-271,W228L}$-*FLO*11$^{214-1360}$-T_{FLO11} in YCplac33	This work
BHUM1581	P_{FLO11}-*FLO*11$^{1-25}$-*FLO*5$^{26-271,N224A}$-*FLO*11$^{214-1360}$-T_{FLO11} in YCplac33	This work
BHUM1583	P_{FLO11}-*FLO*11$^{1-25}$-*FLO*5$^{26-271,Q98A}$-*FLO*11$^{214-1360}$-T_{FLO11} in YCplac33	This work
BHUM1585	P_{FLO11}-*FLO*11$^{1-25}$-*FLO*5$^{26-271,K194A}$-*FLO*11$^{214-1360}$-T_{FLO11} in YCplac33	This work
pET-28a(+)	P_{T7} 6×*His lacI Kan*^{R}	Merck, Germany
pME2519	P_{FLO11}-*FLO*11-T_{FLO11} in YCplac33	(1)

DNA primers

Primer	Sequence 5′ to 3′
FLO11-1	AAAGAGCTCAGTTGGAAAACCCAAAGCCG
FLO11-4	AAAGAGCTCTAATGATACAATTCCAACATGTTCG
FLO11-5	AAAGAGCTCATAGATTGTGACAACAATTGTGCTCCAGTACC
FLO11-6	AAAGAGCTCTGCAGTTGGAAAACCCAAAGCTGAG
FLO5-1	AAAGAGCTCACAGAGGCGTGCTTACCAGC
FLO5-2	AAAGAGCTCACTACTAGCACTATCACAACTACCACC
FLO5-3	AAAGAGCTCATGTATTGAAGGATCAGGGATAG
FLO5-4	AAAGAGCTCAATAATTGCCAGCAATAAGGAC
FLO5-5	AAAGGATCCGCCAGTTCTTTAGTGATTACAGG
FLO5-6	ATTGAATTCGAAGTGTTGTTTGC
FLO5-AA23	CCATATGTCAGGAGCCACAGAGGCG
FLO5-AA271	ACTCGAGTTAATGTATTGAAGGATCAGGGATAGTAC
FLO5^{D160A,D161A}-1	TTTGCAACAGTAGCTGCTTCTGCAATTTTA
FLO5^{D160A,D161A}-2	TAAAATTGCAGAAGCAGCTACTGTTGCAAA
FLO5^{D202T}-1	GAAGTCTCCCTACCAATATCACAGG
FLO5^{D202T}-2	CCTGTGATATTGGTAGGGAGACTTC
FLO5^{K194A}-1	CAATGGTATCGCGCCATGGGATG
FLO5^{K194A}-2	CATCCCATGGCGCGATACCATTG
FLO5^{N224A}-1	GTTGTTTACTCCGCTGCCGTTTCC
FLO5^{N224A}-2	GGAAACGGCAGCGGAGTAAACAAC
FLO5^{Q98A}-1	TTCCTTGTCCTGCAGAAGATTCCTA
FLO5^{Q98A}-2	TAGGAATCTTCTGCAGGACAAGGAA
FLO5^{S227A}-1	CAATGCCGTTGCCTGGGGCACGC
FLO5^{S227A}-2	GCGTGCCCCAGGCAACGGCATTG
FLO5^{W228L}-1	GCCGTTTCCTTGGGCACGCTTC
FLO5^{W228L}-2	GAAGCGTGCCCAAGGAAACGGC
FLO5^{Y222F}-1	CTGAAGGTTGTTTTCTCCAATGCCG
FLO5^{Y222F}-2	CGGCATTGGAGAAAACAACCTTCAG

Table S2. Data collection statistics for Flo5A and its complexes

	Flo5A WT 1 M mannose	Flo5A WT no Ca^{2+}, no sugar	Flo5A WT Man5(D2-D3)	Flo5A WT α1,2-mannobiose	Flo5A WT Man3(D1)	Flo5A S227A α1,2-mannobiose	Flo5A D202T 2 M glucose
X-ray source	ID29, ESRF	ID14-4, ESRF	ID14-2, ESRF	ID14-2, ESRF	ID14-2, ESRF	FR591/CuK_α	FR591/CuK_α
Wavelength (Å)	0.9149	0.9755	0.933	0.933	0.933	1.5418	1.5418
Cell dimensions (Å)	$a = 46.28$, $b = 61.82$, $c = 106.26$	$a = 47.27$, $b = 61.58$, $c = 106.01$	$a = 46.46$, $b = 61.91$, $c = 106.43$	$a = 46.45$, $b = 61.96$, $c = 106.53$	$a = 46.32$, $b = 62.01$, $c = 106.36$	$a = 46.27$, $b = 62.57$, $c = 105.77$	$a = 46.45$, $b = 62.36$, $c = 106.19$
Resolution (Å)	40.29-0.95 (1.00-0.95)	40.16-1.35 (1.42-1.35)	19.43-1.25 (1.32-1.25)	19.44-1.24 (1.30-1.24)	19.39-1.20 (1.26-1.20)	19.40-1.67 (1.76-1.67)	19.42-1.74 (1.83-1.74)
Observed reflections	790095	303038	913485	295380	443365	125571	216633
Unique reflections	190329	64748	85499	82470	93590	35802	32352
Completeness (%)	99.3 (95.7)	96.6 (89.3)	99.8 (99.2)	93.7 (72.4)	97.4 (99.9)	98.2 (93.9)	99.8 (99.3)
Multiplicity	4.2 (3.7)	4.7 (4.3)	10.7 (7.9)	3.6 (3.2)	4.7 (4.6)	3.5 (3.4)	6.7 (6.2)
Mean$I$/sigma(I)	19.6 (2.8)	23.4 (5.2)	21.0 (3.6)	20.5 (2.9)	16.7 (4.7)	18.4 (5.0)	12.6 (2.8)
R_{merge} (%)	2.9 (43.7)	3.6 (28.8)	7.0 (59.3)	3.6 (44.4)	4.4 (33.0)	5.1 (27.2)	11.8 (66.5)

Values for the highest resolution shell are shown in parentheses.

Table S3. Refinement statistics for Flo5A and its complexes

	Flo5A WT 1 M mannose	Flo5A WT no Ca^{2+}, no sugar	Flo5A WT Man5(D2-D3)	Flo5A WT α1, 2-mannobiose	Flo5A WT Man3(D1)	Flo5A S227A α1, 2-mannobiose	Flo5A D202T 2 M glucose
Resolution (Å)	20.00-0.95	20.00-1.35	19.35-1.25	19.44-1.30	19.33-1.20	19.40-1.70	19.36-1.74
R_{work}/R_{free} (%)	10.5/12.2	14.2/17.8	11.4/14.0	12.3/15.2	13.0/15.3	16.4/19.7	18.1/21.9
Reflections							
Total	186922	63557	83938	72600	91841	33558	31755
Test set	3390	1178	1561	1374	1710	624	593
No. of atoms							
Total	2900	2402	2665	2576	2609	2538	2330
Water	460	308	428	410	388	434	292
mean B value (Å^2)	12.246	12.646	10.392	11.452	11.664	15.914	17.120
R.m.s deviations							
Bond lengths (Å)	0.014	0.014	0.012	0.012	0.012	0.013	0.012
Bond angles (°)	1.752	1.524	1.815	1.992	1.457	1.689	1.261